

# NASA TECHNICAL MEMORANDUM

NASA TM X-73552

NASA TM X-73552

(NASA-TM-X-73552) FLIGHT EFFECTS ON EXHAUST  
NOISE FOR TURBOJET AND TURBOFAN ENGINES:  
COMPARISON OF EXPERIMENTAL DATA WITH  
PREDICTION (NASA) 21 p HC A02/MF A01

N77-17062

CSCI 20A G3/07

Unclas  
14885

## FLIGHT EFFECTS ON EXHAUST NOISE FOR TURBOJET AND TURBOFAN ENGINES - COMPARISON OF EXPERIMENTAL DATA WITH PREDICTION

by James R. Stone  
Lewis Research Center  
Cleveland, Ohio 44135



TECHNICAL PAPER to be presented at the  
Ninety-second Meeting of the  
Acoustical Society of America  
San Diego, California, November 16-19, 1976

**FLIGHT EFFECTS ON EXHAUST NOISE FOR TURBOJET  
AND TURBOFAN ENGINES - COMPARISON OF  
EXPERIMENTAL DATA WITH PREDICTION**

by James R. Stone

Lewis Research Center  
National Aeronautics and Space Administration  
Cleveland, Ohio

**ABSTRACT**

Recent experiments on the effects of flight on jet engine exhaust noise have produced apparently conflicting results. Some of these results do not agree with projections based on classical jet noise theories nor with experimental results from model jet simulated flight tests. It has been shown that in some of the cases reported, the proper corrections were not made to account for the distributed nature of the jet noise sources. It is shown herein that the remaining discrepancies can be reconciled by considering the combined effects of jet-mixing noise, internally-generated engine exhaust noise, and shock noise. This paper demonstrates that static and in-flight jet engine exhaust noise can be predicted with reasonable accuracy when the multiple-source nature of the problem is taken into account. Jet-mixing noise is predicted from an improved version of the NASA interim prediction method. Provisional methods of estimating internally-generated noise and shock noise flight effects are used, based partly on existing prediction methods and partly on recently reported engine data.

**INTRODUCTION**

To assess the environmental impact of aircraft noise it is necessary to predict the effect of flight on jet engine exhaust noise. For new or proposed airplanes particularly, such predictions will be based at least in part on model and full-scale static and simulated-flight tests. Because of costs, to rely solely on full-scale flight tests would severely limit the number of configurations and concepts that could be tested. Therefore, it is essential to be able to predict flight noise from static or simulated-flight data.

Some flight data published in the last two years (e.g., refs. 1 and 2) on jet engine exhaust noise do not agree with projections based on classical theory (e.g., ref. 3) or flight simulation experiments (e.g., refs. 4 to 8) for jet-mixing noise. The in-flight levels were found to exceed extrapolated static levels over a wide range of angles, particularly the forward quadrant, while theories such as that of reference 3 and simulation experiments indicated that flight effects should reduce the noise at all angles. It was subsequently shown (ref. 9) that these apparently anomalous flight effects can be largely reconciled on the basis of the combined contributions of jet-mixing noise and internally-generated exhaust noise. It has also been suggested that, in some of the anomalous cases reported, proper accounting of the distributed nature of the noise source was not made in extrapolation of the static data.<sup>(1)</sup> When such corrections are made the apparent anomalies are reduced<sup>(2)</sup>, and even better agreement is obtained between experimental data and predicted values.

More recently reported flight tests (e.g., refs. 10 to 12) indicate a wide range of results. In some cases, an in-flight noise increase in the forward quadrant was observed, while in some cases (e.g., ref. 10) in-flight noise reductions were observed at all angles. Depending on the circumstances, the forward quadrant noise increase has been attributed to shock noise and/or internally-generated noise (e.g., ref. 9). It is of interest to note that there is found spectral evidence of internally-generated noise effects in the flight data of reference 10, even under conditions where the internally-generated noise levels were not sufficient to cause a forward quadrant noise increase. In reference 13, it is indicated that nacelle boundary layer effects can eliminate the source-strength reduction for jet-mixing noise in flight, such as early theories (e.g., ref. 3) predict. Coupled with dynamic effects, this could lead to a forward quadrant noise increase in flight.

It is the purpose of this paper to show that static and in-flight jet engine exhaust noise can be predicted with reasonable accuracy when the multiple-source nature of the problem is taken into account, as has already been

---

(1) Session IV - Discussion (H. S. Ribner, Chairman), Workshop on Effects of Forward Velocity on Jet Noise, NASA Langley Research Center, Hampton, Virginia, Jan. 16, 1976.

(2) "727/JT8D Jet and Fan Noise Flight Effects Study," presented by S. J. Cowan at Workshop on Effects of Forward Velocity on Jet Noise, NASA Langley Research Center, Hampton, Virginia, Jan. 15, 1976.

shown (ref. 9) for a turbojet. The analysis of reference 9 is updated and extended to turbofan engines. Jet-mixing noise is predicted, statically and in-flight, from an improved version of the NASA interim prediction method given in reference 14. Provisional methods of estimating internally-generated noise and shock noise flight effects are used, based partly on existing prediction methods (refs. 15 and 16) and partly on recently reported engine data. The source strength of the internally-generated noise is assumed to be unaffected by flight, as has been observed in small-scale free jet experiments (e. g. , ref. 17). It is further assumed that the internally-generated noise is subject to the convective amplification of a simple noise source,  $-40 \log (1 - M_o \cos \theta)$  (refs. 18 to 20).

### PREDICTION METHODS

The noise of a jet engine, in the absence of dominant fan and compressor noise, is considered herein to be the anti-logarithmic sum of the noises from three uncorrelated sources:

$$\text{SPL} = 10 \log \left( 10^{\text{SPL}_J/10} + 10^{\text{SPL}_{\text{Sh}}/10} + 10^{\text{SPL}_I/10} \right) \quad (1)$$

where the subscript J denotes jet-mixing noise, the subscript I denotes internally-generated noise, and the subscript Sh denotes shock noise (absent for subsonic or fully-expanded supersonic jets). The methods used to predict the noises from these sources are described in the following sections.

#### Jet-Mixing Noise

The jet-mixing noise, in the static case, is predicted using the NASA interim prediction method for jet noise (ref. 14). For the in-flight case only a minor modification (to be described later) to the method of references 9 and 14 has been made herein. The equations will be given here for the OASPL only; spectral prediction curves are given in reference 14. The relations given here are for a single jet; the increments due to the bypass flow are given in reference 14 and are not effected by flight.

Static OASPL<sub>J</sub>. - The overall sound pressure level at a radiation angle,  $\theta$ , of  $90^\circ$  (referred to the engine inlet axis) for shock-free circular jets at ISA ambient conditions is given by

$$\text{OASPL}_{J, 90^\circ} = 141 + 10 \log \left[ \frac{A_j (\rho_j)^w}{R^2 (\rho_a)} \right] + 10 \log \frac{(V_j/c_a)^{7.5}}{1 + 0.01(V_j/c_a)^{4.5}} \quad (2)$$

where

$$w = \frac{3(V_j/c_a)^{3.5}}{0.6 + (V_j/c_a)^{3.5}} - 1 \quad (2a)$$

The  $\text{OASPL}_J$  at other radiation angles is then determined from the following:

$$\text{OASPL}_{J, \theta} - \text{OASPL}_{J, 90^\circ} = -30 \log \left[ 1 + M_c \left( 1 + M_c^5 \right)^{-1/5} \cos \theta \right] + F(\theta') \quad (3)$$

where  $F(\theta')$  is an empirical correction factor shown in figure 1, with

$$\theta' = \theta (V_j/c_a)^{0.1} \quad (3a)$$

and

$$M_c = 0.62(V_j/c_a) \quad (3b)$$

The variations in spectral shape with radiation angle are given in reference 14.

Effects of flight. - To predict the effects of flight on jet-mixing noise, three effects are considered, as listed below:

- (a) Source strength alternation,  $\Delta\text{OASPL}_S$ , due to the effect of the external flow field around the jet plume,
- (b) The dynamic effect,  $\Delta\text{OASPL}_D$ , due to the change in the relative velocity of the source with respect to the propagation medium,
- (c) The kinematic effect,  $\Delta\text{OASPL}_K$ , due to the motion of the airplane with respect to the stationary observer. (This effect was not included in refs. 9 and 14.)

These effects are calculated by the following equations:

$$\Delta \text{OASPL}_S = 10 \log \left\{ \left( 1 - \frac{V_o}{V_j} \right)^{5.625} \frac{1 + 0.01(V_j/c_a)^{4.5}}{1 + 0.01 \left[ (V_j/c_a)(1 - V_o/V_j)^{3/4} \right]^{4.5}} \right\} \\ + 10 \left\{ \frac{3 \left[ (V_j/c_a)(1 - V_o/V_j)^{3/4} \right]^{3.5}}{0.6 + \left[ (V_j/c_a)(1 - V_o/V_j)^{3/4} \right]^{3.5}} - \frac{3(V_j/c_a)^{3.5}}{0.6 + (V_j/c_a)^{3.5}} \right\} \log (\rho_j/\rho_a) \quad (4)$$

$$\Delta \text{OASPL}_D = -30 \log \frac{1 + M_{c,F} \left( 1 + M_{c,F}^5 \right)^{-1/5} \cos \theta}{1 + M_{c,S} \left( 1 + M_{c,S}^5 \right)^{-1/5} \cos \theta} \quad (5)$$

where  $M_{c,S}$  is calculated from equation (3b) and  $M_{c,F}$  is given by

$$M_{c,F} = 0.62(V_j - V_o)/C_a \quad (5a)$$

$$\Delta \text{OASPL}_K = -10 \log \left[ 1 - (V_o/c_a) \cos \theta \right] \quad (6)$$

Spectral effects are predicted on the basis of similarity at constant  $f/(V_j - V_o)$ , where  $V_o = 0$  in the static case, as well as a Doppler frequency shift.

### Internally-Generated Noise

Static OASPL<sub>I</sub>. - The internally-generated noise from a jet engine arises from many sources, such as combustion noise, turbomachinery noise, and flow noise. In the present analysis, the acoustics of these sources is lumped, and the prediction is based on the core noise parameters used in references 15 and 16. First, the peak noise, at  $\theta = 120^\circ$ , is calculated from the following equation:

$$\text{OASPL}_{I, 120^\circ} = K_I - 20 \log R + 10 \log \left\{ \dot{m} \left[ (T_4 - T_3) \left( \frac{P_3}{P_a} \right) \left( \frac{T_a}{T_3} \right) \right]^2 \right\} \quad (7)$$

where  $K_I = 56$  for turbojets and 46 for turbofans. For comparison reference 15 indicates  $K_I = 47.1$  for both turbojets and turbofans, while reference 16 indicates  $K_I = 57.4$  for turbojets and 41.4 for turbofans. (The values of  $K_I$  are applicable using the S.I. units of this paper; in U.S. customary units the values of  $K_I$  should be 1.1 dB higher.)

The variation of  $\text{OASPL}_I$  (referred to that at  $\theta = 120^\circ$ ) with angle is shown in figure 2 for several engines (refs. 16, 21, and 22) as well as for combustors (ref. 16). The prediction method of references 15 and 21 and that of reference 16 are shown for comparison. Considerable scatter is evident in the experimental data. The prediction methods, being based on different sets of data, are also not in close agreement. The prediction curve used herein (solid line) is intermediate between these two earlier prediction curves and is largely based on examination of the data of reference 23.

Effect of flight. - When an acoustic source is in motion its radiation characteristics are altered. Ahead of the moving source, the intensity of the sound is increased, and behind the moving source the intensity of the sound is decreased, while at  $90^\circ$  from the axis of the moving source there is no effect. These effects result from source motion relative to both the observer (kinematic effect) and the propagation medium (dynamic effect).

The effect of source motion relative to the observer is due to the well-known Doppler effect. Additionally, the sound intensity is amplified by the Doppler factor  $(1 - M_o \cos \theta)^{-1}$ . The effect of source motion relative to the medium on sound intensity may be approximated by the Doppler factor raised to a power dependent on the type of source. Thus, the combined kinematic and dynamic effects may be lumped. The following expression is used in this report:

$$\text{OASPL}_{I, F} - \text{OASPL}_{I, S} = -40 \log(1 - M_o \cos \theta) \quad (8)$$

This is consistent with the recent empirical analysis of flight data reported in reference 10, as well as with the theory of Morse and Ingard (ref. 18) for a moving monopole and with the theory of Lighthill (ref. 19) for a moving dipole.

This formulation (eq. (8)) has been suggested by Dorsch (ref. 20) for jet-flap interaction noise, where the noise source moves with the airplane, as is the case for internally-generated noise. It should be noted, however, that Lighthill (ref. 19) suggests that  $-20 \log(1 - M_o \cos \theta)$  should be used for a moving monopole; and internally-generated noise may well consist of both monopole (combustion) and dipole (flow-surface interaction) noises.

Spectral shape. - The spectral shape referred to in reference 16 as the "spectral envelope" is used herein. Reference 16 indicates that a narrower spectrum is recommended for pure combustion noise. However, in an engine all the internal sources are dealt with, so the broader "spectral envelope," which agrees with engine data reasonably well, is more appropriate for the present study. The peak of the spectrum is at 400 Hz statically (as in ref. 16); in flight a Doppler frequency shift is assumed.

#### Shock-Associated Noise

No new method of predicting shock-associated noise is proposed herein. Instead, static experimental data are used as a base for the prediction of in-flight shock noise. The effects of flight are assumed to be the same as for internally-generated noise.

#### COMPARISON OF PREDICTION WITH EXPERIMENTAL FLIGHT DATA

In order to illustrate some typical effects of flight on jet engine exhaust noise, the following typical shock free case, taken from reference 9, is chosen as an example: a single-engine airplane with  $V_j/c_a = 1.8$ ,  $\rho_j/\rho_a = 0.3$ , and  $M_o = 0.35$ . The results of the prediction of the separate jet-mixing and internally-generated noises, as well as their sum, are shown as a function of angle in figure 3, for both the static and in-flight cases. Considering first the static case (fig. 3(a)), it can be seen that the jet noise is dominant at all angles. The total noise, obtained by addition of internally-generated and jet-mixing noises, differs very little from the jet noise, and in an experiment could easily be interpreted as being pure jet noise.

In flight (fig. 3(b)), the jet noise is reduced at all angles (but more so in the rear quadrant than the front quadrant) while the internally-generated noise is increased for  $\theta < 90^\circ$  and decreased for  $\theta > 90^\circ$ . Thus, in flight the internally-generated noise is dominant for  $\theta < 95^\circ$ . It can then be seen



that the apparent dominance of jet noise statically does not indicate that at the same jet velocity or engine power, jet noise will be dominant in flight, as has often been assumed (e. g., ref. 2). The total noise levels statically and in flight are compared in figure 3(c). The in-flight noise exceeds the static noise for  $\theta < 60^\circ$ ; this is quite similar to much of the flight data (e. g., ref. 1). It is apparent that this forward quadrant noise increase is dependent on the relative levels of internally-generated noise (and/or shock noise) and jet-mixing noise, as will be shown in the comparisons which follow.

### Turbofan Engines

To demonstrate the validity of the prediction methods used in this study, the first comparisons made are between static data and the prediction methods. Then experimental and predicted flight noise levels and static-to-flight increments are compared.

Static. - Experimental and predicted OASPL directivity patterns (on a 4.57-m radius) are compared in figure 4 for a refanned JT8D turbofan engine (ref. 23).<sup>(3)</sup> Data are shown for three different primary jet velocities. The agreement is very good for the two highest velocities, with the peak noise levels agreeing within less than 1 dB. At the lower jet velocity the noise is slightly over-predicted at all angles, and the peak noise is over-estimated by 2.8 dB. (However, on a sideline basis this difference is reduced to 1.2 dB as will be shown later.) In all cases, the jet-mixing noise is predicted to exceed the internally generated noise at all angles, as shown in the spectral comparisons which follow.

Experimental and predicted spectra are compared in figure 5 for a refanned JT8D engine at the intermediate primary jet velocity ( $V_j/c_a = 1.18$ ). Comparisons are made at  $\theta = 150^\circ$  (peak noise angle at constant radius, fig. 5(a)),  $\theta = 90^\circ$  (fig. 5(b)), and  $\theta = 50^\circ$  (fig. 5(c)). Good agreement is shown at all angles. Jet-mixing noise is the dominant source throughout all

---

<sup>(3)</sup> These data were obtained from isolated-nacelle engine stand tests, but 3 dB has been added for later comparison with flight data for the two-engine DC-9 airplane.

these spectra, according to the prediction methods<sup>(4)</sup> and<sup>for</sup> both the higher and lower jet velocities (not shown).

Flight. - Experimental and predicted flyover directivity patterns are compared in figure 6 for a Douglas DC-9 airplane with refanned JT8D engines. Static levels projected to flight are also shown; these are the data of figure 4 re-plotted on a sideline basis. The angular scale used is weighted to give a time-history shape (the scale is linear in  $\text{ctn } \theta$ ). Although there is some disagreement at large angles ( $>3$  dB), the peak in-flight levels are predicted within  $\pm 1$  dB, and the agreement at angles before the peak is excellent. Thus, it can be seen that in-flight noise levels can be predicted with reasonable accuracy, and the problem area is in the rear quadrant rather than the forward quadrant. Improved rear quadrant predictions may require a modification in the  $F(\theta')$  term shown in figure 1.

The corresponding experimental and predicted in-flight spectra are shown for the intermediate jet velocity in figure 7. Comparisons again are made at  $\theta = 150^\circ$  (fig. 7(a)),  $\theta = 90^\circ$  (fig. 7(b)), and  $\theta = 50^\circ$  (fig. 7(c)). Jet-mixing noise is predicted to be the more important source at all angles, but the internally-generated noise contribution is significant, especially at  $\theta = 90^\circ$  and  $\theta = 50^\circ$ . The general agreement of experimental and predicted data is encouraging, but the previously indicated problem in the rear quadrant is again evident. As indicated before, the only change needed in the prediction may be in evaluation of  $F(\theta')$  for large  $\theta'$ . However, at the highest jet velocity of reference 23 only the  $\theta = 150^\circ$  spectral data were shown, and the agreement of those data with prediction is better than that shown in figure 7(a). For the lowest primary jet velocity, corresponding spectral comparisons are shown in figure 8. In this case the internally-generated noise is predicted to be dominant at all angles, and the agreement with prediction is good for all cases.

Static-to-flight increments. - Experimental and predicted static-to-flight increments are shown in figure 9. The refanned JT8D/DC-9 data, which have been shown in more detail in the preceding sections, are shown in figure 9(a), and data for a Boeing 727 airplane with conventional JT8D engines<sup>(5)</sup> are shown

<sup>(4)</sup> Absolute values of the internally-generated noise prediction parameters of eq. (7) were not given in ref. 23, but it was shown that the predicted internally-generated noise varied approximately with the third power of primary jet velocity. The levels shown here are extrapolated from low jet velocity data using this velocity dependence and should agree closely with eq. (7).

<sup>(5)</sup> Boeing presentation, "727/JT8D Jet and Fan Noise Flight Effects Study," Oral Report No. 1, Contract DOT FA71WA-2637, Mod. 12.

in figure 9(b). Since these comparisons involve subtracting two experimental values to obtain each data point, the apparent discrepancies between experimental and predicted values are magnified. The two sets of data show comparable worst-case disagreements of about  $\pm 3.5$  dB, which should be considered good for comparisons of this type. The trends in the experimental data are predicted rather well, but in figure 9(b) there is a consistent overprediction of the in-flight noise reduction, which amounts to as much as  $\sim 2$  dB in the forward quadrant.

### Turbojet Engines

The contention that internally-generated noise must be taken into account in predicting in-flight exhaust noise was first demonstrated for a turbojet engine in reference 9. As additional evidence, experimental and predicted static-to-moving OASPL increments are shown in figure 10 for a J85 engine installed on the Bertin aerotrain (experimental data of ref. 11). Data for simulated-flight Mach numbers of 0.12 and 0.24 are shown in figures 10(a) and 10(b), respectively. At the highest jet velocity, shock noise is predicted to have a significant effect which is absent at the two lower jet velocities. (The observed excess static noise above that predicted for jet-mixing and internally-generated noises was projected to flight assuming it to be a shock-associated noise.) Except for radiation angles of  $140^\circ$  or greater in rear quadrant, the agreement is even better here than for the turbofan engines (fig. 9). Further study is required to determine to what extent this large-angle problem is due to shortcomings of the prediction methods and how much error may be due to experimental inaccuracies.

### Discussion

As can be seen from the results shown herein, the type of static-to-flight effects to be expected depends on the relative levels of jet-mixing noise and internally-generated noise (and/or shock noise). To demonstrate this point directly, static and flight experimental and predicted flyover directivity patterns are compared in figure 11 for engines with different levels of internally-generated noise relative to jet-mixing noise. Data for the Viper 610 turbojet engine in an HS-125 airplane (at low jet velocity,  $V_j/c_a \approx 1.0$ ) (ref. 1) are shown in figure 11(a) and represent a "high" internal noise case.

Data for refanned JT8D engines in a DC-9 airplane (at high jet velocity,  $V_j/c_a \approx 1.4$ ) (ref. 23) are shown in figure 11(b) and represent a "low" internal noise case. For the high internal noise case (fig. 11(a)) a forward quadrant noise increase in flight is predicted and observed, while for the low internal noise case (fig. 11(b)) noise reductions are predicted and observed at all angles.

### CONCLUDING REMARKS

This paper has shown that static and in-flight jet engine exhaust noise can be predicted with reasonable accuracy when the multiple-source nature of the problem is taken into account. It has also been shown that the apparently conflicting static-to-flight increments for various tests can be reconciled when the relative levels of jet-mixing, internally-generated, and shock-associated noises are considered.

### APPENDIX - SYMBOLS

$A_j$	fully-expanded primary jet area, $m^2$
$c_a$	ambient sonic velocity, $m/sec$
$f$	1/3-octave-band center frequency, $Hz$
$F(\theta')$	jet noise directivity correction (fig. 1), $dB$ re $20 \mu N/m^2$
$K_I$	constant in internally-generated noise prediction, $dB$ re $20 \mu N/m^2$
$L$	perpendicular distance from observer to flight path, $m$
$\dot{m}$	mass flow rate, $kg/sec$
$M_c$	convection Mach number, $0.62 (V_j - V_o)/c_a$ , dimensionless
$M_o$	flight Mach number, $V_o/c_a$ , dimensionless
OASPL	overall sound pressure level, $dB$ re $20 \mu N/m^2$
$\Delta OASPL$	change in OASPL with flight, $OASPL_F - OASPL_S$ , $dB$
$P$	total pressure, $N/m^2$
$R$	source-to-observer distance, $m$
SPL	1/3-octave-band sound pressure level, $dB$ re $20 \mu N/m^2$

T	total temperature, K
$V_j$	primary jet velocity (isentropic, fully expanded), m/sec
$V_o$	airplane velocity, m/sec
w	density ratio exponent, dimensionless
$\rho_j$	fully-expanded jet density, kg/m <sup>3</sup>
$\rho_a$	ambient density, kg/m <sup>3</sup>
$\theta$	polar angle from flight path, deg
$\theta'$	effective angle, $\theta(V_j/c_a)^{0.1}$ , deg

## Subscripts:

a	ambient
D	dynamic
F	flight
I	internally generated
J	jet mixing
K	kinematic
S	static
Sh	shock associated
$\theta$	evaluation at $\theta$
$90^\circ$	evaluation at $\theta = 90^\circ$
$120^\circ$	evaluation at $\theta = 120^\circ$
3	combustor inlet
4	combustor exit

## REFERENCES

1. Brooks, J. R. and Woodrow, R. J. (1975). "The Effects of Forward Speed on a Number of Turbojet Exhaust Silencers," AIAA Paper 75-506.
2. Bushell, K. W. (1975). "Measurement and Prediction of Jet Noise in Flight," AIAA Paper 75-461.

3. Ffowcs Williams, J. E. (1963). "The Noise from Turbulence Convected at High Speed," *Phil. Trans. Roy. Soc. (London)* 255, 469-503.
4. von Glahn, U. H., Groesbeck, D. E., and Goodykoontz, J. H. (1973). "Velocity Decay and Acoustic Characteristics of Various Nozzle Geometries with Forward Velocity," *AIAA Paper* 73-629.
5. Packman, A. B., Ng, K. W., and Paterson, R. W. (1975). "Effects of Simulated Forward Flight on Subsonic Jet Exhaust Noise," *AIAA Paper* 75-869.
6. Cocking, B. J. and Bryce, W. D. (1975). "Subsonic Jet Noise in Flight Based on Some Recent Wind-Tunnel Results," *AIAA Paper* 75-462.
7. Plumblee, H. E., Jr. (Ed.) (1976). "Effects of Forward Velocity on Turbulent Jet Mixing Noise," *NASA CR-2702*.
8. Cocking, B. J. (1976). "The Effect of Flight on Subsonic Jet Noise," *AIAA Paper* 76-555.
9. Stone, J. R. (1975). "On the Effects of Flight on Jet Engine Exhaust Noise," *NASA TM X-71819*.
10. Merriman, J. E., et al. (1976). "Forward Motion and Installation Effects on Engine Noise," *AIAA Paper* 76-584.
11. Clapper, W. S., et al. (1976). "Development of a Technique for Jet Noise Simulation. I, II," *AIAA Paper* 76-532.
12. Drevet, P., Duponchel, J. P., and Jacques, J. R. (1976). "Effect on Flight on the Noise from a Convergent Nozzle as Observed on the Bertin Aerotraine," *AIAA Paper* 76-557.
13. Sarohia, V. and Massier, P. F. (1976). "Effects of External Boundary Layer Flow on Jet Noise in Flight," *AIAA Paper* 76-558.

15. Huff, R. G., Clark, B. J., and Dorsch, R. G. (1974). "Interim Prediction Method for Low Frequency Core Engine Noise," NASA TM X-71627.
16. Motsinger, R. E. and Emmerling, J. J. (1975). "Review of Theory and Methods for Combustion Noise Prediction," AIAA Paper 75-541.
17. von Glahn, U. and Goodykoontz, J. (1973). "Forward Velocity Effects on Jet Noise with Dominant Internal Noise Source," paper presented at 86th Meeting of the Acoust. Soc. Am., Los Angeles, Calif., Paper Z5.
18. Morse, P. M. and Ingard, K. U. (1968). Theoretical Acoustics (McGraw-Hill, New York).
19. Lighthill, M. J. (1962). "The Bakerian Lecture, 1961. Sound Generated Aerodynamically," Proc. Roy. Soc. (London), A267, 147-182.
20. Dorsch, R. G. (1974). "Externally Blown Flap Noise Research," SAE Paper 740468.
21. Dunn, D. G. and Peart, N. A. (1973). "Aircraft Noise Source and Contour Estimation," Boeing Commercial Airplane Co. Rept. D6-60233; also NASA CR-114649.
22. (1975). "Response to Notice of Proposed Rule Making for the Control of the Noise of Civil Supersonic Airplanes (Docket No. 10494; Notice No. 75-15). Annex 2: Jet Exhaust Silencer Evaluation. An Appraisal of Model and Full Scale Noise Data with Particular Reference to Forward Speed Effects and Simulation," Rolls-Royce Ltd. (Bristol Engine Div.) Rept. GML/JDV/47091.
23. (1975). "DC-9 Flight Demonstration Program with Refanned JT8D Engines. Volume 4: Flyover Noise," Douglas Aircraft Co., Inc. Rept. MDC-J4518-vol-4; also NASA CR-134860.

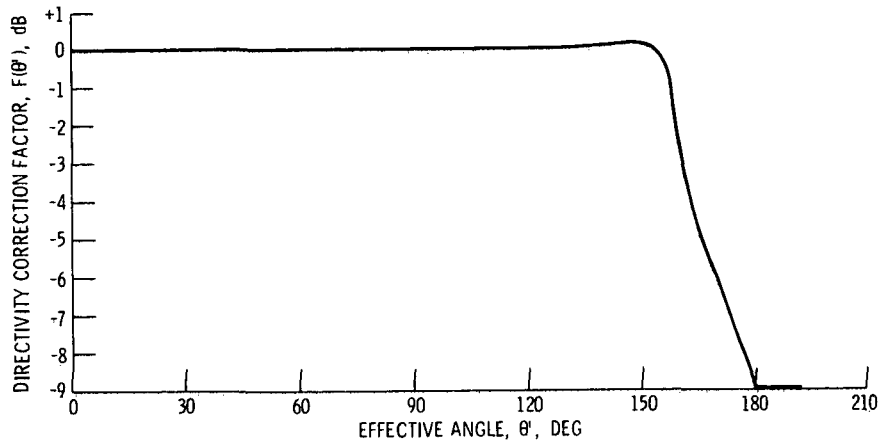


Figure 1. - Directivity correction factor as function of effective angle for jet noise prediction of references 9 and 14.

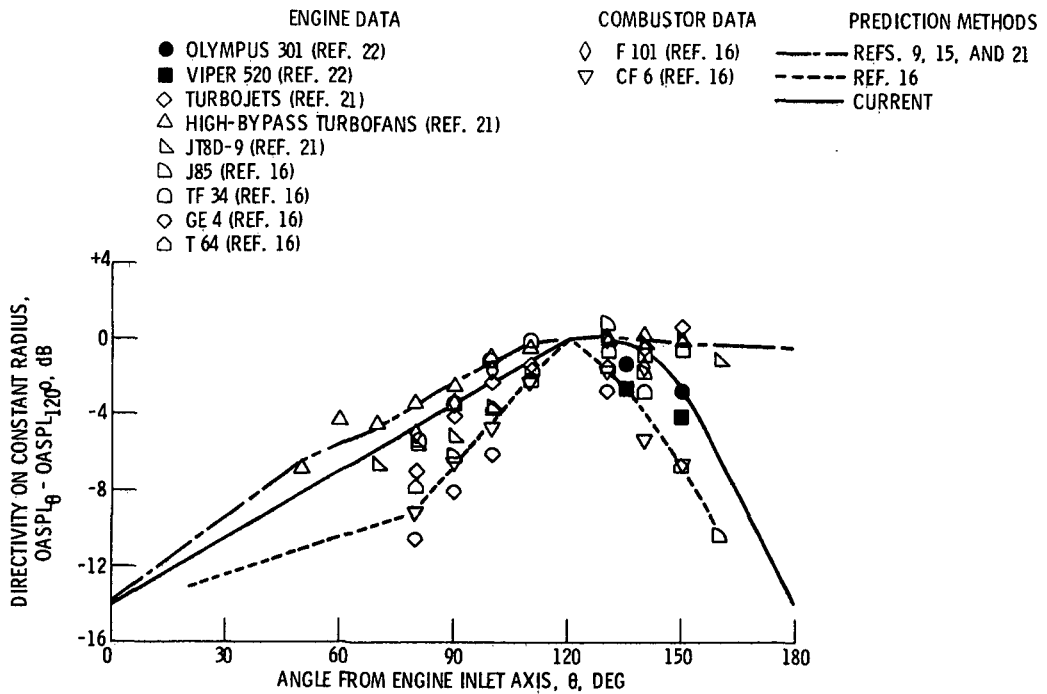


Figure 2. - Internally-generated noise static directivity-comparison of data with prediction methods.

ORIGINAL PAGE IS  
OF POOR QUALITY

PRECEDING PAGE BLANK NOT FILMED



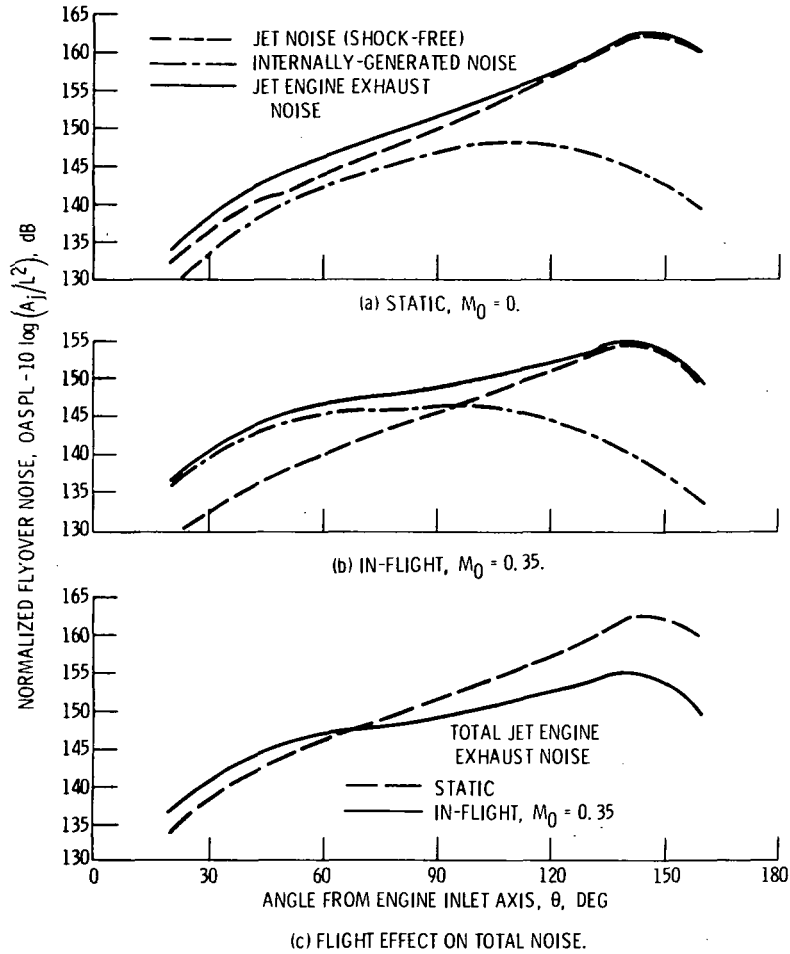


Figure 3. - Synthesis of jet engine exhaust noise directivity for typical jet engine, with  $V_j/c_a = 1.80$ .

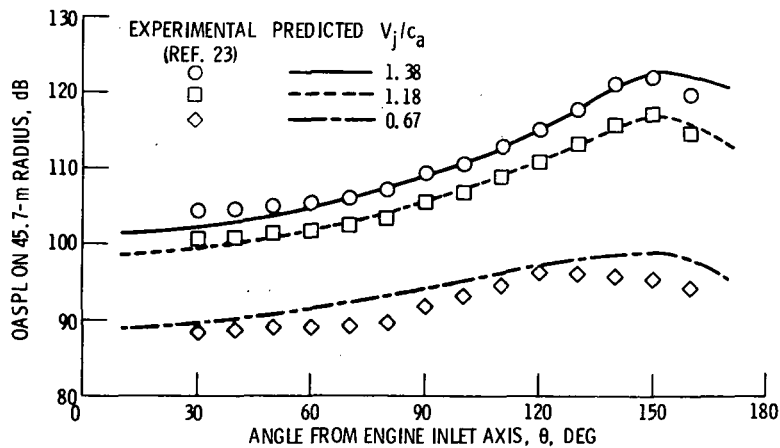


Figure 4. - Comparison of experimental data with prediction of OASPL directivity for static engine-stand tests of a refanned JT8D turbofan engine.

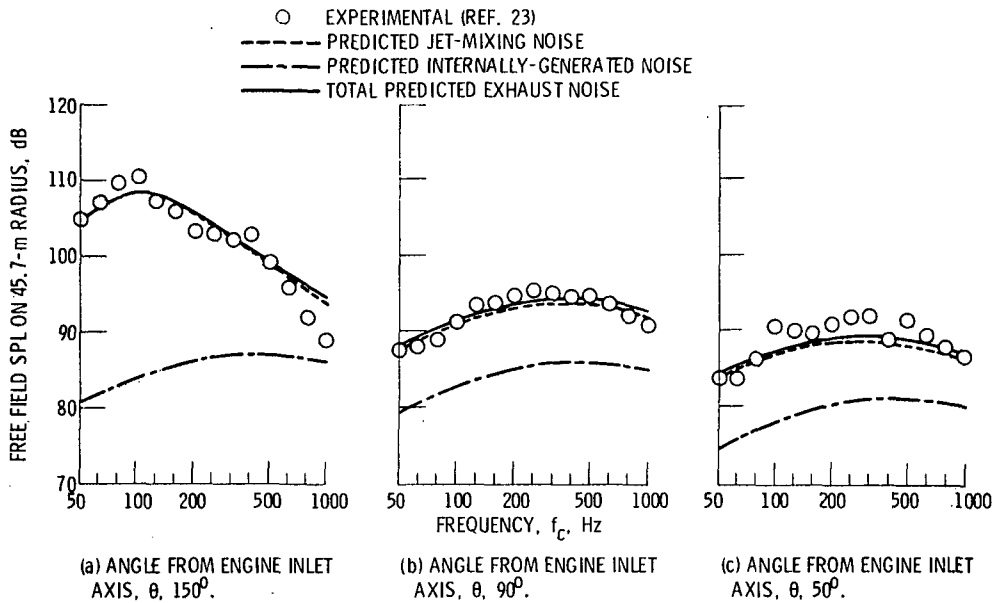


Figure 5. - Comparison of experimental and predicted SPL spectra for static engine-stand tests of a re-fanned turbofan JT8D engine; intermediate jet velocity,  $V_j/c_a = 1.18$ .

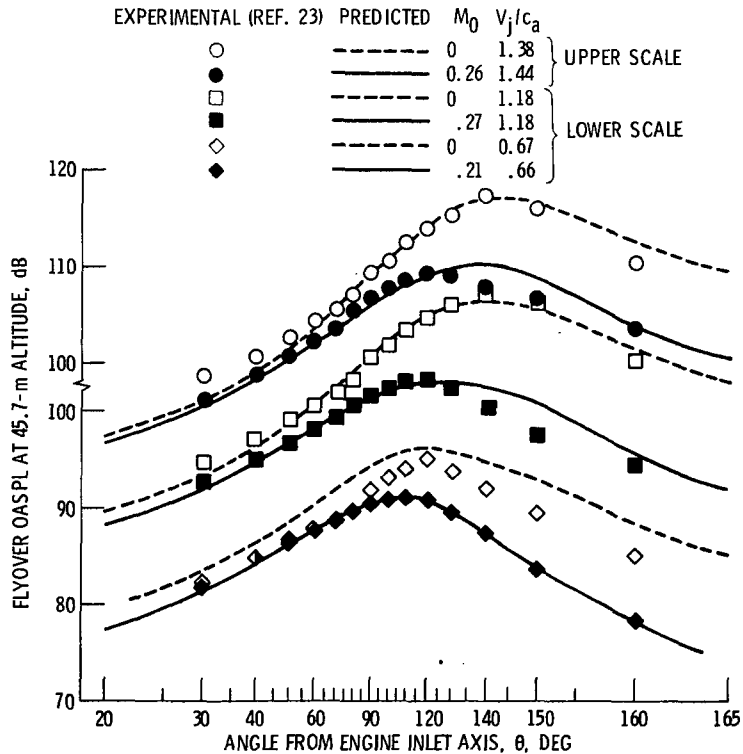


Figure 6. - Comparison of flyover and projected static OASPL directivities with prediction for a DC-9 airplane with two re-fanned JT8D turbofan engines.

ORIGINAL PAGE IS  
 OF POOR QUALITY

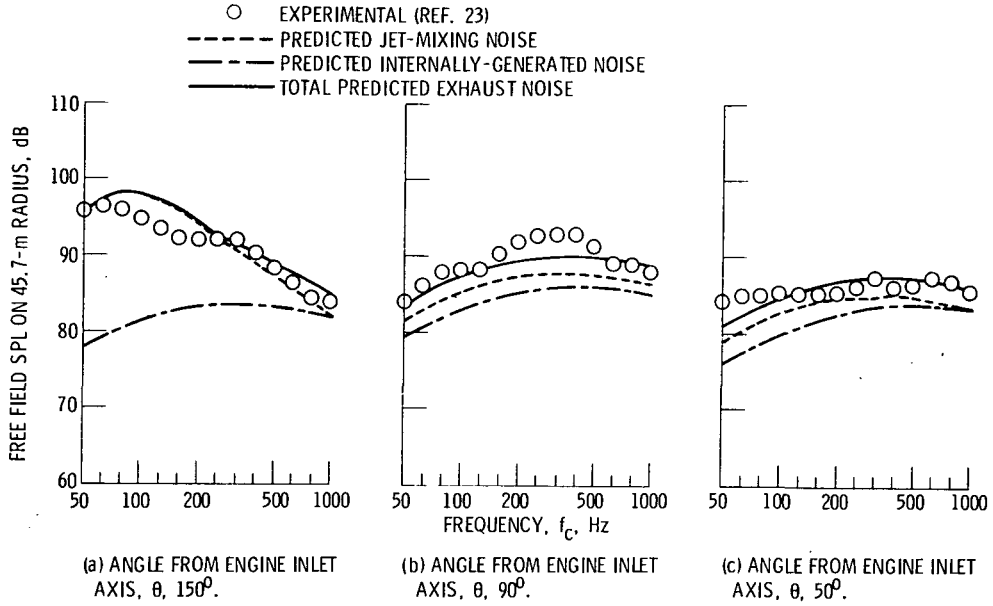


Figure 7. - Comparison of experimental and predicted flight SPL spectra for a DC-9 airplane with two re-fanned JT8D turbofan engines; intermediate jet velocity,  $V_j/c_a = 1.18$ ; flight Mach number,  $M_0$ , 0.27.

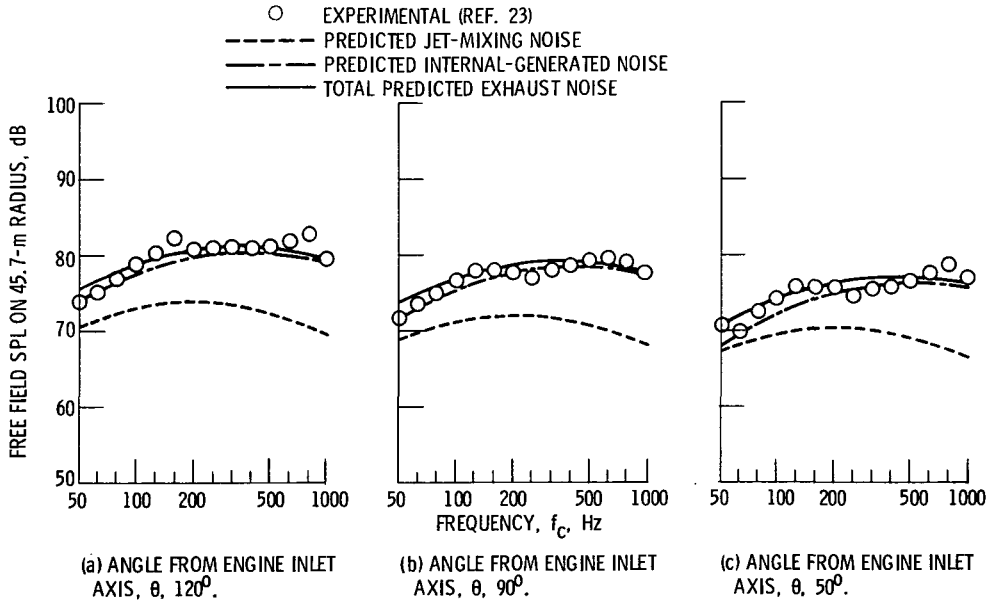
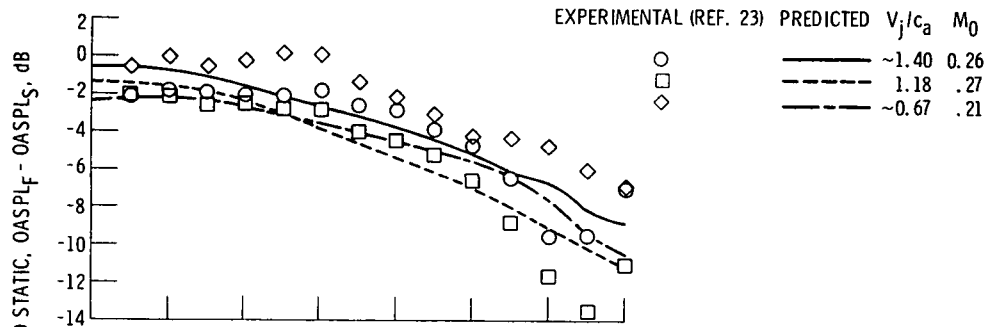
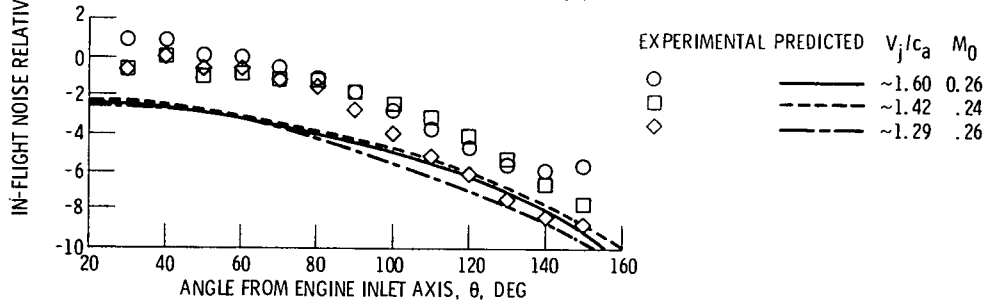


Figure 8. - Comparison of experimental and predicted flight SPL spectra for a DC-9 airplane with two re-fanned JT8D turbofan engines; low jet velocity,  $V_j/c_a = 0.66$ ; flight Mach number,  $M_0$ , 0.21.

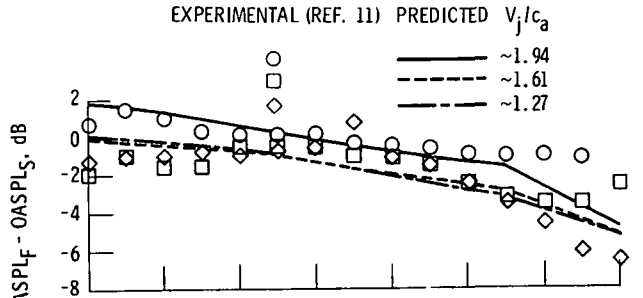


(a) DC-9 AIRPLANE WITH TWO REFINED JT8D ENGINES.

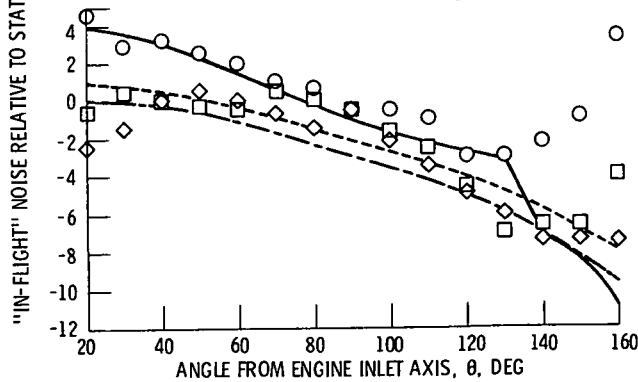


(b) 727 AIRPLANE WITH THREE CONVENTIONAL JT8D ENGINES.

Figure 9. - Comparison of experimental and predicted static-to-flight OASPL increments as a function of angle for turbofan engines.



(a) AEROTRAIN MACH NUMBER,  $M_0 \sim 0.12$ .



(b) AEROTRAIN MACH NUMBER,  $M_0 \sim 0.24$ .

Figure 10. - Comparison of experimental and predicted static-to-moving OASPL increments as a function of angle for a J85 turbojet engine on the Bertin Aerotrain.

ORIGINAL PAGE IS  
OF POOR QUALITY

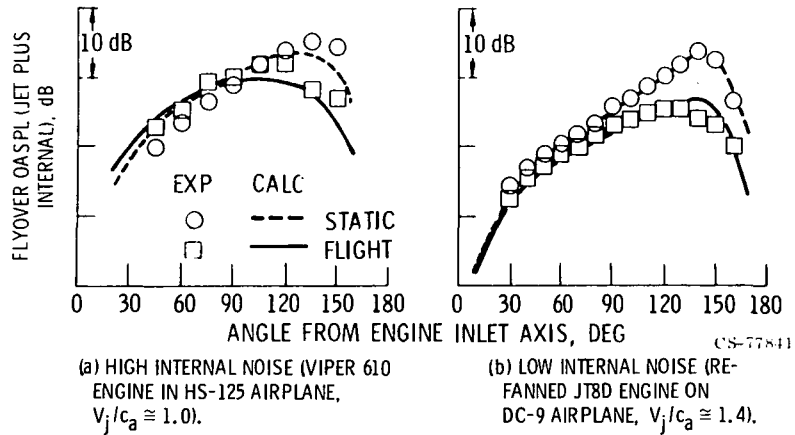


Figure 11. - Comparison of calculated and measured static and flight directivities for engines with different levels of internal noise relative to jet noise.